ARTICLE IN PRESS

Journal of Computational and Applied Mathematics ▮ (▮▮▮▮) ▮▮▮–▮▮▮

Contents lists available at ScienceDirect

Journal of Computational and Applied Mathematics

journal homepage: www.elsevier.com/locate/cam

Operator splitting for the numerical solution of free surface flow at low capillary numbers

Giovanna Guidoboni [a,*], Roland Glowinski [a,b], Matteo Pasquali [c,d,e]

[a] Department of Mathematics, University of Houston, Houston, TX 77204-3476, USA
[b] Laboratoire Jacques-Louis Lions, Université P. et M. Curie, 4 Place Jussieu, 75005, Paris, France
[c] Department of Chemical & Biomolecular Engineering, Rice University, Houston, TX, 77251-1892, USA
[d] Department of Chemistry, Rice University, Houston, TX, 77251-1892, USA
[e] Ken Kennedy Institute for Information Technology, Rice University, Houston, TX, 77251-1892, USA

ARTICLE INFO

Article history:
Received 19 April 2007
Received in revised form 16 December 2007

Dedicated to Hideo Kawarada on the occasion of his 70th birthday

Keywords:
Free surface flow
Operator splitting
Low capillary number

ABSTRACT

Free surface flows are pervasive in engineering and biomedical applications. In many interesting cases—particularly when small length scales are involved—surface forces (capillarity) dominate the flow dynamics. In these cases, computing the flow together with the shape of the surfaces, requires specialized solution techniques. This article investigates the capabilities of an operator splitting/finite elements method at handling accurately incompressible viscous flow with free surfaces at low capillary numbers. The test case of flow in the downstream section of a slot coater is used for three reasons: (1) it is an established benchmark; (2) it represents an idealized, yet industrially relevant flow; (3) high-fidelity results obtained with monolithic algorithms are available in literature. The flow and free surface shape attained with the new operator splitting scheme agree very satisfactorily with the results obtained with monolithic solvers. Because of its inherent computational simplicity, the new operator splitting scheme is attractive for large-scale simulations, three-dimensional flows, and flows of complex fluids.

Published by Elsevier B.V.

1. Introduction

The numerical simulation of free surface flows has many applications in science and engineering. Examples include coating flows, ink-jet printing and polymer processing. In these applications, the dynamics of the free surface flow is dominated by the competition of surface tension and viscous forces. Strong capillary pressure changes, occur at curved free surfaces; these shape-dependent terms occur in the momentum balance equation through the boundary conditions, and couple the equations of the flow and domain shape very tightly, making their numerical solution difficult [8,9,15].

To date, only fully-coupled algorithms have been shown to be stable and/or accurate when capillary forces dominate—see, e.g., [8,15]. However, these approaches require the solution of a large system of coupled nonlinear algebraic equations, which can become cost-ineffective, particularly for three-dimensional flows.

In this paper, we describe a partitioned algorithm, based on an operator splitting technique, which can be used to solve free surface flows at low capillary numbers, which imply strong capillary effects. The operator splitting technique [2,10] allows us to decouple the nonlinearities of the problem and then treat them independently using suitable numerical solvers, convenient space approximations and different time steps.

* Corresponding author.
E-mail address: gio@math.uh.edu (G. Guidoboni).

0377-0427/$ – see front matter. Published by Elsevier B.V.
doi:10.1016/j.cam.2008.10.051

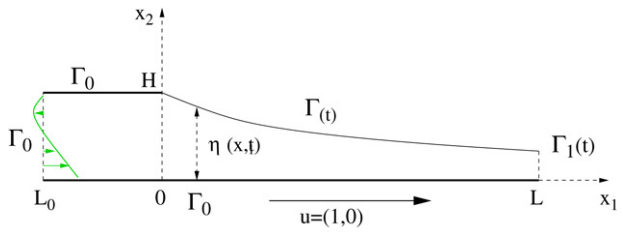

Fig. 1. Sketch of the flow domain in the downstream section of a slot coater.

A careful choice of the methods used to solve each substep is crucial in order to achieve the desired accuracy. The main features of our approach are the following.

(1) The advection steps are solved using a wave-like equation method. This approach has proved to handle successfully both structured and unstructured meshes, and it appears to be less dissipative than the usual method of characteristics, or those based on upwinding [2,4,5,11].
(2) Generalized Stokes problems precede and follow the advection steps, in order to ensure that the velocity field is divergence-free and smooth out the solution. These substeps can be solved via conjugate gradient methods, see e.g. [2].
(3) The time step for each subproblem can be chosen independently and, in particular, a smaller time step is chosen for the advection steps.

This methodology was used in [4] to study Hopf bifurcation for a flow down an inclined plane. In the present article, we show that our splitting algorithm succeeds in computing, with very good accuracy, the steady flow of a Newtonian fluid in a slot coater at capillary number $Ca = 0.1$ (conventional partitioned algorithms fail at $Ca \lesssim 1$ in this problem [15]). The steady profile of the free surface is virtually identical to that computed in Ref. [12] with a monolithic method (and tested against the pioneering work of [14] that introduced fully-coupled ALE-FEM methods).

The paper is organized as follows. In Section 2 we present the mathematical formulation of the problem, while the time and space discretizations are described in Section 3. Numerical experiments are discussed in Section 4.

2. Mathematical formulation

In the downstream section of a slot coater, an incompressible viscous fluid occupies the two-dimensional time-dependent region of space $\Omega(t)$ whose boundary is given by $\partial\Omega(t) = \Gamma_0 \cup \Gamma_1(t) \cup \Gamma(t)$, as shown in Fig. 1. The portion Γ_0 of the boundary is fixed, while $\Gamma(t)$ and $\Gamma_1(t)$ are free surfaces, meaning that they depend on time, and their location is not given a priori.

Let us consider a Cartesian frame of reference (O, x_1, x_2), as shown in Fig. 1. We assume that the free surface $\Gamma(t)$ admits a Cartesian representation at each instant of time so that it can be described by the time-dependent function $\eta(x_1, t)$. This allows us to write

$$\Gamma(t) = \{\mathbf{x} = (x_1, x_2) \in \mathbb{R}^2 : x_1 \in (0, L), x_2 = \eta(x_1, t)\}, \tag{1}$$

$$\Gamma_1(t) = \{\mathbf{x} = (x_1, x_2) \in \mathbb{R}^2 : x_1 = L, x_2 \in (0, \eta(L, t))\}. \tag{2}$$

We remark that $\Gamma_1(t)$ is a vertical segment of variable length.

The fluid flow is modeled by the Navier–Stokes equations

$$\begin{aligned} &\nabla \cdot \mathbf{u} = 0 \quad \text{in } \Omega(t) \times (0, T) \\ &\varrho[\partial_t \mathbf{u} + (\mathbf{u} \cdot \nabla)\mathbf{u}] = \nabla \cdot \boldsymbol{\sigma} + \mathbf{f} \quad \text{in } \Omega(t) \times (0, T), \end{aligned} \tag{3}$$

where $\mathbf{u} = (u_1, u_2)$ is the velocity of the fluid, ϱ is the fluid density, $\boldsymbol{\sigma}$ is the stress tensor defined as $\boldsymbol{\sigma} = -p\mathbf{I} + 2\mu\mathbf{D}(\mathbf{u})$, where p is the pressure, μ is the viscosity and $\mathbf{D}(\mathbf{u}) = (\nabla\mathbf{u} + (\nabla\mathbf{u})^t)/2$ is the rate-of-strain tensor, where the superscript t means transpose, and $\mathbf{f}$ is the external force density. Here ∂_t denotes the partial derivative with respect to time, while $\nabla = (\partial_1, \partial_2)$ is the gradient with respect to the spatial variables.

At Γ_0 we prescribe the velocity of the fluid, while on $\Gamma_1(t)$ we prescribe zero stress, leading to the conditions

$$\mathbf{u} = \mathbf{g}_0 \quad \text{on } \Gamma_0 \times (0, T), \quad \boldsymbol{\sigma}\mathbf{n} = \mathbf{0} \quad \text{on } \Gamma_1(t) \times (0, T), \tag{4}$$

where $\mathbf{g}_0$ is a given function of $\mathbf{x}$ and t.

Remark 1. Several choices are available for the boundary condition at the outlet section $\Gamma_1(t)$. A common choice is to assume fully developed flow, namely $\mathbf{n} \cdot \nabla\mathbf{u} = \mathbf{0}$, as in [12]. In this paper, we use the zero stress condition because it is easier to implement and it leads to similar results as the fully developed flow condition if, at the discrete level, one considers that capillary forces do not act on the corner point at the intersection between $\Gamma(t)$ and $\Gamma_1(t)$.

Please cite this article in press as: G. Guidoboni, et al., Operator splitting for the numerical solution of free surface flow at low capillary numbers, Journal of Computational and Applied Mathematics (2008), doi:10.1016/j.cam.2008.10.051

The free boundary $\Gamma(t)$ represents the interface between the fluid and the external ambient, and it is made of fluid particles. In order to ensure that the fluid particles do not cross the surface, we need the following kinematic condition

$$\partial_t \eta + u_1 \partial_1 \eta - u_2 = 0 \quad \text{on } \Gamma(t) \times (0, T), \quad \text{with } \eta(0, t) = H. \tag{5}$$

An additional condition is needed to establish the balance of stress

$$\boldsymbol{\sigma}\mathbf{n} = s\mathcal{H}(\eta(x_1, t))\mathbf{n} \quad \text{on } \Gamma(t) \times (0, T), \tag{6}$$

where $\mathbf{n} = (-\partial_1\eta, 1)/\sqrt{1 + |\partial_1\eta|^2}$ is the outward unit normal vector, s is the surface tension (which is assumed to be positive and constant), and $\mathcal{H}(\eta(x_1, t)) = \partial_1^2\eta/(1 + |\partial_1\eta|^2)^{3/2}$ is the curvature.

To complete the formulation of the problem, initial conditions should be prescribed for the velocity of the fluid and the shape of the domain:

$$\mathbf{u}(\mathbf{x}, 0) = \mathbf{u}_0(\mathbf{x}) \quad \text{with } \nabla \cdot \mathbf{u}_0 = 0, \quad \eta(x_1, 0) = \eta_0(x_1). \tag{7}$$

In order to write the variational formulation of the problem (3)–(7) we introduce the following functional spaces:

$$V_{\mathbf{g}_0}(\Omega(t)) = \{\mathbf{v} | \mathbf{v} \in (H^1(\Omega(t)))^2, \mathbf{v} = \mathbf{g}_0 \text{ on } \Gamma_0\}, \tag{8}$$

$$V_0(\Omega(t)) = \{\mathbf{v} | \mathbf{v} \in (H^1(\Omega(t)))^2, \mathbf{v} = \mathbf{0} \text{ on } \Gamma_0\}, \tag{9}$$

$$S_H = \{\phi | \phi \in H^1(0, L), \phi(0) = H\}, \tag{10}$$

$$S_0 = \{\phi | \phi \in H^1(0, L), \phi(0) = 0\}. \tag{11}$$

Now, we multiply equations (3)$_1$, (3)$_2$ and (5) by the test functions $q \in L^2(\Omega(t))$, $\mathbf{v} \in V_0(\Omega(t))$ and $\phi \in S_0$, respectively (we use the notation $\varphi(t)$ to denote the function $x \to \varphi(x, t)$). The resulting equations are integrated over $\Omega(t)$ to obtain the variational formulation of (3)–(7):

$$\begin{aligned}
&\textit{For a.e.} t > 0, \textit{find } \mathbf{u}(t) \in V_{\mathbf{g}_0}(\Omega(t)), p(t) \in L^2(\Omega(t)), \ \eta(t) \in S_H \textit{ such that}\\
&\varrho \int_{\Omega(t)} \partial_t \mathbf{u} \cdot \mathbf{v} \, d\mathbf{x} + \varrho \int_{\Omega(t)} (\mathbf{u} \cdot \nabla)\mathbf{u} \cdot \mathbf{v} \, d\mathbf{x} + 2\mu \int_{\Omega(t)} \mathbf{D}(\mathbf{u}) : \mathbf{D}(\mathbf{v}) \, d\mathbf{x}\\
&\quad - \int_{\Omega(t)} p \nabla \cdot \mathbf{v} \, d\mathbf{x} = \int_{\Omega(t)} \mathbf{f} \cdot \mathbf{v} \, d\mathbf{x} + s \int_{\Gamma(t)} \mathcal{H}(\eta(x_1, t))\mathbf{n} \cdot \mathbf{v} \, d\Gamma(t), \quad \forall \mathbf{v} \in V_0(\Omega(t)),\\
&\int_{\Omega(t)} q \nabla \cdot \mathbf{u} \, d\mathbf{x} = 0, \quad \forall q \in L^2(\Omega(t)),\\
&\int_0^L \partial_t \eta \phi \, dx_1 + \int_0^L (u_1|_{\Gamma(t)} \partial_1 \eta - u_2|_{\Gamma(t)})\phi \, dx_1 = 0, \ \forall \phi \in S_0,\\
&\mathbf{u}(\mathbf{x}, 0) = \mathbf{u}_0(\mathbf{x}), \quad \text{with } \nabla \cdot \mathbf{u}_0 = 0, \quad \text{and} \quad \eta(x_1, 0) = \eta_0(x_1).
\end{aligned} \tag{12}$$

Remark 2. Rather than imposing a contact angle between Γ_0 and $\Gamma(t)$, we choose to pin the free surface to mimic the effect of a sharp corner on a surface. At a sharp corner (radius of ~ 25 μm), a liquid can move by a small amount and adjust within a broad range of angles to assume its equilibrium value. This is how contact lines are pinned in practice. Indeed, the velocity field has a discontinuity at the contact line, which induces infinite velocity gradients (and hence stress), see e.g. Fig. 16 in [12]. However, this phenomenon occurs in several well-known problems in computational fluid-dynamics, such as the wall-driven flow in a square cavity. In the cavity flow, the solution loses regularity at the corners and, strictly speaking, the solution is not in H^1. Nevertheless, numerical experiments show that the H^1-theory can be successfully applied for the numerical solution of the flow problem [2,7].

Remark 3. The choice of S_H and S_0 given by (10) and (11) is justified by the following integrations by parts:

$$s \int_{\Gamma(t)} \mathcal{H}(\eta) v_1 n_1 \, d\Gamma(t) = -s \int_0^L (1 + |\partial_1\eta|^2)^{-1/2} \partial_1 v_1 \, dx_1, \tag{13}$$

$$s \int_{\Gamma(t)} \mathcal{H}(\eta) v_2 n_2 \, d\Gamma(t) = -s \int_0^L \partial_1\eta (1 + |\partial_1\eta|^2)^{-1/2} \partial_1 v_2 \, dx_1. \tag{14}$$

Here the x_1-differentiation on η is transferred on the two components of the test function $\mathbf{v}$. Both (13) and (14) assume that $\mathbf{v} \cdot \boldsymbol{\tau} = 0$ at $\Gamma_1(t) \cap \Gamma(t)$, where $\boldsymbol{\tau} = (1, \partial_1\eta)/\sqrt{1 + |\partial_1\eta|^2}$.

Please cite this article in press as: G. Guidoboni, et al., Operator splitting for the numerical solution of free surface flow at low capillary numbers, Journal of Computational and Applied Mathematics (2008), doi:10.1016/j.cam.2008.10.051

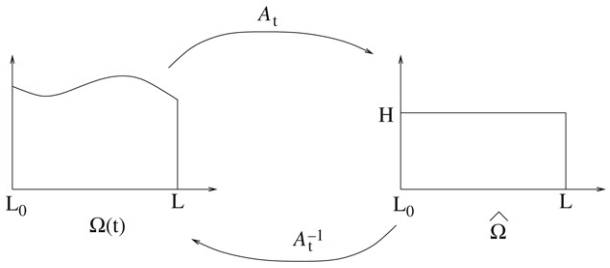

Fig. 2. $\mathcal{A}_t$ maps the the current domain $\Omega(t)$ into the reference domain $\widehat{\Omega}$.

Problem (12) is defined on the domain $\Omega(t)$ which changes in time and is not known a priori. Therefore we are going to reformulate problem (12) into a fixed reference domain.

Let $(\mathcal{A}_t)_{t\in(0,T)}$ be a family of mappings which, at each time $t \in (0, T)$, map the current domain $\Omega(t)$ onto the reference domain $\widehat{\Omega} = (0, L) \times (0, H)$ defined by

$$\mathcal{A}_t : \Omega(t) \subset \mathbb{R}^2 \to \widehat{\Omega} \subset \mathbb{R}^2$$
$$\mathbf{x} = (x_1, x_2) \to \boldsymbol{\xi} = (\xi_1, \xi_2) = \mathcal{A}_t(\mathbf{x}) = \begin{cases} \xi_1 = x_1 \\ \xi_2 = \dfrac{H}{\eta(x_1, t)} x_2, \end{cases} \tag{15}$$

as sketched in Fig. 2. We observe that $\Gamma(t)$ is mapped into

$$\hat{\Gamma} = \{\boldsymbol{\xi} = (\xi_1, \xi_2) \in \mathbb{R}^2 | \xi_1 \in (0, L), \xi_2 = H\}, \tag{16}$$

while $\Gamma_1(t)$ becomes

$$\hat{\Gamma}_1 = \{\boldsymbol{\xi} = (\xi_1, \xi_2) \in \mathbb{R}^2 | \xi_1 = L, \xi_2 \in (0, H)\}. \tag{17}$$

The Jacobian matrix $\mathbf{J}$ of this transformation and its determinant J are given by

$$\mathbf{J} = \mathbf{J}(\eta) = \begin{bmatrix} 1 & 0 \\ -\dfrac{\xi_2}{\eta(\xi_1, t)} \partial_1 \eta(\xi_1, t) & \dfrac{H}{\eta(\xi_1, t)} \end{bmatrix}, \qquad J = J(\eta) = \frac{H}{\eta(\xi_1, t)}. \tag{18}$$

It is clear that this transformation is well defined as long as $\eta(\xi_1, t) > 0$ or, in other words, as long as the free surface does not touch the bottom. Let $f = f(\mathbf{x}, t)$ be a function defined on $\Omega(t)$ and $\hat{f} = \hat{f}(\boldsymbol{\xi}, t) = f(\mathcal{A}_t^{-1}(\boldsymbol{\xi}), t)$ the corresponding function defined on $\widehat{\Omega}$. Due to the change of variables, we have

$$\int_{\Omega(t)} f(\mathbf{x}, t)\, d\mathbf{x} = \int_{\widehat{\Omega}} \hat{f}(\boldsymbol{\xi}, t) J\, d\boldsymbol{\xi}. \tag{19}$$

Moreover, it follows from the chain rule that

$$\partial_t f = \partial_t \hat{f} - \mathbf{w} \cdot \widehat{\nabla} \hat{f}, \tag{20}$$

where $\widehat{\nabla} = \mathbf{J}^{-t} \nabla$ and the domain velocity $\mathbf{w}$ is given by

$$\begin{aligned} \mathbf{w}(\boldsymbol{\xi}, t) &= \partial_t \boldsymbol{\xi} = \frac{\xi_2}{\eta(\xi_1, t)} \partial_t \eta(\xi_1, t) \mathbf{e}_2 \\ &= \frac{\xi_2}{\eta(\xi_1, t)} \left[u_2(\xi_1, \eta(\xi_1, t), t) - u_1(\xi_1, \eta(\xi_1, t), t) \partial_1 \eta(\xi_1, t) \right] \mathbf{e}_2. \end{aligned} \tag{21}$$

The last step is a consequence of the kinematic condition (5) and we used the notation $\mathbf{e}_2 = (0, 1)$.

Using (19) and (20), problem (12) becomes:

For a.e. $t > 0$, *find* $\hat{\mathbf{u}}(t) \in V_{\mathbf{g}_0}(\widehat{\Omega})$, $\hat{p}(t) \in L^2(\widehat{\Omega})$, $\eta(t) \in S_H$, such that

$$\begin{aligned} &\varrho \int_{\widehat{\Omega}} \partial_t \hat{\mathbf{u}} \cdot \hat{\mathbf{v}} J(\eta)\, d\boldsymbol{\xi} - \varrho \int_{\widehat{\Omega}} (\mathbf{w} \cdot \widehat{\nabla}) \hat{\mathbf{u}} \cdot \hat{\mathbf{v}} J(\eta)\, d\boldsymbol{\xi} + \varrho \int_{\widehat{\Omega}} (\hat{\mathbf{u}} \cdot \widehat{\nabla}) \hat{\mathbf{u}} \cdot \hat{\mathbf{v}} J(\eta)\, d\boldsymbol{\xi} \\ &\quad + 2\mu \int_{\widehat{\Omega}} \hat{\mathbf{D}}(\hat{\mathbf{u}}) : \hat{\mathbf{D}}(\hat{\mathbf{v}}) J(\eta)\, d\boldsymbol{\xi} - \int_{\widehat{\Omega}} \hat{p} \widehat{\nabla} \cdot \hat{\mathbf{v}} J(\eta)\, d\boldsymbol{\xi} = \int_{\widehat{\Omega}} \hat{\mathbf{f}} \cdot \hat{\mathbf{v}} J(\eta)\, d\boldsymbol{\xi} \end{aligned}$$

$$+s\int_0^L \mathcal{H}(\eta)\left(\hat{v}_2(\xi_1,H)-\hat{v}_1(\xi_1,H)\partial_1\eta\right)\,\mathrm{d}\xi_1,\quad \forall\hat{\mathbf{v}}\in V_0(\widehat{\Omega}),$$

$$\int_{\widehat{\Omega}}\hat{q}\widehat{\nabla}\cdot\hat{\mathbf{u}}J(\eta)\,\mathrm{d}\boldsymbol{\xi}=0,\quad \forall\hat{q}\in L^2(\widehat{\Omega}),$$

$$\int_0^L\partial_t\eta\phi\,\mathrm{d}\xi_1+\int_0^L(\hat{u}_1(\xi_1,H,t)\partial_1\eta-\hat{u}_2(\xi_1,H,t))\phi\,\mathrm{d}\xi_1=0,\quad\forall\phi\in S_0,$$

$$\hat{\mathbf{u}}(\boldsymbol{\xi},0)=\hat{\mathbf{u}}_0(\boldsymbol{\xi}),\quad\text{with }\widehat{\nabla}\cdot\hat{\mathbf{u}}_0=0,\quad\text{and}\quad\eta(\xi_1,0)=\eta_0(\xi_1).\tag{22}$$

Here we used the notation $\hat{\mathbf{D}}(\hat{\mathbf{u}})=(\widehat{\nabla}\hat{\mathbf{u}}+(\widehat{\nabla}\hat{\mathbf{u}})^t)/2$.

3. Time and space discretizations

The numerical solution of problem (21) contains three main difficulties: (a) the incompressibility condition and the related unknown pressure, (b) an advection term associated to the velocity of the fluid, (c) an advection term associated to the velocity of the domain. The difficulty associated with the unknown location of the free boundary has been removed through the transformation defined by (15). A time discretization by operator splitting allows to decouple the difficulties of the problem and to treat each of them with an appropriate method. Moreover it makes it possible to update the location of the free boundary as a sub-step, avoiding costly sub-iterations between the location of the free surface and the solution of the Navier–Stokes equations. Among the many possible versions, we advocate a very simple operator splitting method which is first-order accurate [10]. The low order accuracy is compensated, actually, by easy implementation and less cost in computational time.

Let Δt be the time discretization step and $t^n=n\Delta t$, $\hat{\mathbf{u}}^n=\hat{\mathbf{u}}(t^n)$, $\hat{p}^n=\hat{p}(t^n)$, $\eta^n=\eta(t^n)$. For $n\geq 0$, $\hat{\mathbf{u}}^n$ and η^n being known, the scheme consists of solving the following problems.

(1) Find $\hat{\mathbf{u}}^{n+1/5}\in V_{\mathbf{g}_0}(\widehat{\Omega})$ and $\hat{p}^{n+1/5}\in L^2(\widehat{\Omega})$ such that

$$\begin{cases}\varrho\displaystyle\int_{\widehat{\Omega}}\frac{\hat{\mathbf{u}}^{n+1/5}-\hat{\mathbf{u}}^n}{\Delta t}\cdot\hat{\mathbf{v}}J(\eta^n)\,\mathrm{d}\boldsymbol{\xi}+\mu\int_{\widehat{\Omega}}\hat{\mathbf{D}}(\hat{\mathbf{u}}^{n+1/5}):\hat{\mathbf{D}}(\hat{\mathbf{v}})J(\eta^n)\,\mathrm{d}\boldsymbol{\xi}\\ \quad-\int_{\widehat{\Omega}}\hat{p}^{n+1/5}\widehat{\nabla}\cdot\hat{\mathbf{v}}J(\eta^n)\,\mathrm{d}\boldsymbol{\xi}=\int_{\widehat{\Omega}}\hat{\mathbf{f}}^{n+1}\cdot\hat{\mathbf{v}}\,J(\eta^n)\,\mathrm{d}\boldsymbol{\xi}\\ \quad+s\int_0^L\mathcal{H}(\eta^n)\left(\hat{v}_2(\xi_1,H)-\hat{v}_1(\xi_1,H)\partial_1\eta^n\right)\,\mathrm{d}\xi_1,\quad\forall\hat{\mathbf{v}}\in V_0(\widehat{\Omega}),\\ \displaystyle\int_{\widehat{\Omega}}\hat{q}\widehat{\nabla}\cdot\hat{\mathbf{u}}^{n+1/5}J(\eta^n)\,\mathrm{d}\boldsymbol{\xi}=0,\quad\forall\hat{q}\in L^2(\widehat{\Omega}).\end{cases}\tag{23}$$

(2) Find $\hat{\mathbf{u}}^{n+2/5}\in V(\widehat{\Omega})$ via the solution of the following pure advection problem in $\widehat{\Omega}\times(t^n,t^{n+1})$

$$\begin{cases}\displaystyle\int_{\widehat{\Omega}}\partial_t\hat{\mathbf{u}}\cdot\hat{\mathbf{v}}J(\eta^n)\,\mathrm{d}\boldsymbol{\xi}+\int_{\widehat{\Omega}}(\hat{\mathbf{u}}^{n+1/5}\cdot\widehat{\nabla})\hat{\mathbf{u}}\cdot\hat{\mathbf{v}}J(\eta^n)\,\mathrm{d}\boldsymbol{\xi}=0,\quad\forall\hat{\mathbf{v}}\in\widehat{V}^{n+1/5,-},\\ \hat{\mathbf{u}}(t^n)=\hat{\mathbf{u}}^{n+1/5},\\ \hat{\mathbf{u}}(t)=\hat{\mathbf{u}}^{n+1/5}\quad\text{on}\quad\partial\widehat{\Omega}^{n+1/5,-}\times(t^n,t^{n+1}),\end{cases}\tag{24}$$

and then set $\hat{\mathbf{u}}^{n+2/5}=\hat{\mathbf{u}}(t^{n+1})$. The functional spaces introduced here are defined as follows

$$V(\widehat{\Omega})=\{\mathbf{v}|\mathbf{v}\in(H^1(\widehat{\Omega}))^2\},$$
$$\widehat{V}^{n+1/5,-}=\{\mathbf{v}|\mathbf{v}\in(H^1(\widehat{\Omega}))^2,\mathbf{v}=\mathbf{0}\quad\text{on}\quad\partial\widehat{\Omega}^{n+1/5,-}\},$$
$$\partial\widehat{\Omega}^{n+1/5,-}=\{\boldsymbol{\xi}|\boldsymbol{\xi}\in\partial\widehat{\Omega},\hat{\mathbf{u}}^{n+1/5}(\boldsymbol{\xi})\cdot\hat{\mathbf{n}}(\boldsymbol{\xi})<0\}.$$

(3) Find $\hat{\mathbf{u}}^{n+3/5}\in V_{\mathbf{g}_0}(\widehat{\Omega})$ and $\hat{p}^{n+3/5}\in L^2(\widehat{\Omega})$ such that

$$\begin{cases}\varrho\displaystyle\int_{\widehat{\Omega}}\frac{\hat{\mathbf{u}}^{n+3/5}-\hat{\mathbf{u}}^{n+2/5}}{\Delta t}\cdot\hat{\mathbf{v}}J(\eta^n)\,\mathrm{d}\boldsymbol{\xi}+\mu\int_{\widehat{\Omega}}\hat{\mathbf{D}}(\hat{\mathbf{u}}^{n+3/5}):\hat{\mathbf{D}}(\hat{\mathbf{v}})J(\eta^n)\,\mathrm{d}\boldsymbol{\xi}\\ -\displaystyle\int_{\widehat{\Omega}}\hat{p}^{n+3/5}\widehat{\nabla}\cdot\hat{\mathbf{v}}J(\eta^n)\,\mathrm{d}\boldsymbol{\xi}=0,\quad\forall\hat{\mathbf{v}}\in V_0(\widehat{\Omega}),\\ \displaystyle\int_{\widehat{\Omega}}\hat{q}\widehat{\nabla}\cdot\hat{\mathbf{u}}^{n+3/5}J(\eta^n)\,\mathrm{d}\boldsymbol{\xi}=0,\quad\forall\hat{q}\in L^2(\widehat{\Omega}).\end{cases}\tag{25}$$

(4) Find $\hat{\mathbf{u}}^{n+4/5}\in V(\widehat{\Omega})$ via the solution of the following pure advection problem in $\widehat{\Omega}\times(t^n,t^{n+1})$

$$\begin{cases}\displaystyle\int_{\widehat{\Omega}}\partial_t\hat{\mathbf{u}}\cdot\hat{\mathbf{v}}J(\eta^n)\,\mathrm{d}\boldsymbol{\xi}-\int_{\widehat{\Omega}}(\mathbf{w}^{n+3/5}\cdot\widehat{\nabla})\hat{\mathbf{u}}\cdot\hat{\mathbf{v}}J(\eta^n)\,\mathrm{d}\boldsymbol{\xi}=0,\quad\forall\hat{\mathbf{v}}\in\widehat{W}^{n+3/5,+},\\ \hat{\mathbf{u}}(t^n)=\hat{\mathbf{u}}^{n+3/5},\\ \hat{\mathbf{u}}(t)=\hat{\mathbf{u}}^{n+3/5}\quad\text{on}\quad\partial\widehat{\Omega}^{n+3/5,+}\times(t^n,t^{n+1}),\end{cases}\tag{26}$$

and then set $\hat{\mathbf{u}}^{n+4/5} = \hat{\mathbf{u}}(t^{n+1})$ and $\hat{p}^{n+4/5} = \hat{p}^{n+1/5} + \hat{p}^{n+3/5}$. Here

$$\mathbf{w}^{n+3/5}(\boldsymbol{\xi}) = \frac{\xi_2}{\eta^n(\xi_1)}\left[\hat{u}_2^{n+3/5}(\xi_1, H) - \hat{u}_1^{n+3/5}(\xi_1, H)\partial_1\eta^n(\xi_1)\right]\mathbf{e}_2, \tag{27}$$

and

$$\widehat{W}^{n+3/5,+} = \{\mathbf{v}|\mathbf{v} \in (H^1(\widehat{\Omega}))^2, \mathbf{v} = \mathbf{0} \quad \text{on} \quad \partial\widehat{\Omega}^{n+3/5,+}\},$$
$$\partial\widehat{\Omega}^{n+3/5,+} = \{\boldsymbol{\xi}|\boldsymbol{\xi} \in \partial\widehat{\Omega}, \mathbf{w}^{n+3/5}(\boldsymbol{\xi}) \cdot \hat{\mathbf{n}}(\boldsymbol{\xi}) > 0\}.$$

(5) Find the new position of the free surface $\eta^{n+1} \in S_H$ by solving the following problem in $(0, L) \times (t^n, t^{n+1})$

$$\begin{cases} \displaystyle\int_0^L \partial_t\eta\phi \, \mathrm{d}\xi_1 + \int_0^L (\hat{u}_1^{n+4/5}(\xi_1, H)\partial_1\eta - \hat{u}_2^{n+4/5}(\xi_1, H))\phi \, \mathrm{d}\xi_1 = 0, \quad \forall\phi \in S_0, \\ \eta(\xi_1, t^n) = \eta^n(\xi_1). \end{cases} \tag{28}$$

The new physical domain Ω^{n+1} is obtained from the reference domain $\widehat{\Omega}$ through the mapping $\mathcal{A}_{t^{n+1}}^{-1}$ defined as:

$$\mathcal{A}_{t^{n+1}}^{-1} : \widehat{\Omega} \subset \mathbb{R}^2 \to \Omega^{n+1} \subset \mathbb{R}^2$$
$$\boldsymbol{\xi} = (\xi_1, \xi_2) \to \mathbf{x} = (x_1, x_2) = \begin{cases} x_1 = \xi_1 \\ x_2 = \dfrac{\eta^{n+1}(\xi_1)}{H}\xi_2. \end{cases} \tag{29}$$

The velocity $\mathbf{u}^{n+1}$ and the pressure p^{n+1} defined on the new domain Ω^{n+1} are obtained as follows

$$\begin{aligned} \mathbf{u}^{n+1}(x_1, x_2) &= \hat{\mathbf{u}}^{n+4/5}(x_1, Hx_2/\eta^{n+1}(x_1)), \\ p^{n+1}(x_1, x_2) &= \hat{p}^{n+4/5}(x_1, Hx_2/\eta^{n+1}(x_1)), \end{aligned} \tag{30}$$

where $(x_1, x_2) \in \Omega^{n+1}$.

We remark that in (23)–(26) $\widehat{\nabla} = \mathbf{J}^{-t}(\eta^n)\nabla$ and that, indeed, it is much easier to solve the sub-problems (23)–(25) in their equivalent formulation in the physical domain Ω^n (which is fixed from the way the problem was split). Moreover, problems (23) and (25) can be significantly simplified by noticing that

$$\mu\int_{\Omega(t)} \mathbf{D}(\mathbf{u}) : \mathbf{D}(\mathbf{v}) \, \mathrm{d}\mathbf{x} = \frac{\mu}{2}\int_{\Omega(t)} \nabla\mathbf{u} : \nabla\mathbf{v} \, \mathrm{d}\mathbf{x} + \frac{\mu}{2}\int_{\Omega(t)} (\nabla\mathbf{u})^t : \nabla\mathbf{v} \, \mathrm{d}\mathbf{x}, \tag{31}$$

and then evaluating the last integral in (31) at the previous fractional step. Problems (23)-(25) are then modified as follows.

(1) Find $\mathbf{u}^{n+1/5} \in V_{\mathbf{g}_0}(\Omega^n)$ and $p^{n+1/5} \in L^2(\Omega^n)$ such that

$$\begin{cases} \varrho\displaystyle\int_{\Omega^n} \frac{\mathbf{u}^{n+1/5} - \mathbf{u}^n}{\Delta t} \cdot \mathbf{v} \, \mathrm{d}\mathbf{x} + \frac{\mu}{2}\int_{\Omega^n} \nabla\mathbf{u}^{n+1/5} : \nabla\mathbf{v} \, \mathrm{d}\mathbf{x} - \int_{\Omega^n} p^{n+1/5}\nabla \cdot \mathbf{v} \, \mathrm{d}\mathbf{x} \\ \quad = s\displaystyle\int_{\Gamma^n} \mathcal{H}(\eta^n)\mathbf{n} \cdot \mathbf{v} \, \mathrm{d}\Gamma^n + \int_{\Omega^n} \mathbf{f}^{n+1} \cdot \mathbf{v} \, \mathrm{d}\mathbf{x} - \frac{\mu}{2}\int_{\Omega^n} (\nabla\mathbf{u}^n)^t : \nabla\mathbf{v} \, \mathrm{d}\mathbf{x}, \quad \forall\mathbf{v} \in V_0(\Omega^n), \\ \displaystyle\int_{\Omega^n} q\nabla \cdot \mathbf{u}^{n+1/5} \, \mathrm{d}\mathbf{x} = 0, \quad \forall q \in L^2(\Omega^n). \end{cases} \tag{32}$$

(2) Find $\mathbf{u}^{n+2/5} \in V(\Omega^n)$ via the solution of the following pure advection problem in $\Omega^n \times (t^n, t^{n+1})$

$$\begin{cases} \displaystyle\int_{\Omega^n} \partial_t\mathbf{u} \cdot \mathbf{v} \, \mathrm{d}\mathbf{x} + \int_{\Omega^n} (\mathbf{u}^{n+1/5} \cdot \nabla)\mathbf{u} \cdot \mathbf{v} \, \mathrm{d}\mathbf{x} = 0, \quad \forall\mathbf{v} \in V^{n+1/5,-}, \\ \mathbf{u}(t^n) = \mathbf{u}^{n+1/5}, \\ \mathbf{u}(t) = \mathbf{u}^{n+1/5} \quad \text{on} \quad \partial\Omega^{n+1/5,-} \times (t^n, t^{n+1}), \end{cases} \tag{33}$$

and then set $\mathbf{u}^{n+2/5} = \mathbf{u}(t^{n+1})$. The functional spaces introduced here are defined as follows

$$V(\Omega^n) = \{\mathbf{v}|\mathbf{v} \in (H^1(\Omega^n))^2\},$$
$$V^{n+1/5,-} = \{\mathbf{v}|\mathbf{v} \in (H^1(\Omega^n))^2, \mathbf{v} = \mathbf{0} \quad \text{on} \quad \partial\Omega^{n+1/5,-}\},$$
$$\partial\Omega^{n+1/5,-} = \{\mathbf{x}|\mathbf{x} \in \partial\Omega^n, \mathbf{u}^{n+1/5}(\mathbf{x}) \cdot \mathbf{n}(\mathbf{x}) < 0\}.$$

Please cite this article in press as: G. Guidoboni, et al., Operator splitting for the numerical solution of free surface flow at low capillary numbers, Journal of Computational and Applied Mathematics (2008), doi:10.1016/j.cam.2008.10.051

(3) Find $\mathbf{u}^{n+3/5} \in V_{\mathbf{g}_0}(\Omega^n)$ and $p^{n+3/5} \in L^2(\Omega^n)$ such that

$$\begin{cases} \varrho \displaystyle\int_{\Omega^n} \frac{\mathbf{u}^{n+3/5} - \mathbf{u}^{n+2/5}}{\Delta t} \cdot \mathbf{v}\, d\mathbf{x} + \frac{\mu}{2} \int_{\Omega^n} \nabla \mathbf{u}^{n+3/5} : \nabla \mathbf{v}\, d\mathbf{x} - \int_{\Omega^n} p^{n+3/5} \nabla \cdot \mathbf{v}\, d\mathbf{x} \\ \quad = -\dfrac{\mu}{2} \displaystyle\int_{\Omega^n} (\nabla \mathbf{u}^{n+2/5})^t : \nabla \mathbf{v}\, d\mathbf{x}, \quad \forall \mathbf{v} \in V_0(\Omega^n), \\ \displaystyle\int_{\Omega^n} q \nabla \cdot \mathbf{u}^{n+3/5}\, d\mathbf{x} = 0, \quad \forall q \in L^2(\Omega^n). \end{cases} \tag{34}$$

Then we define $\hat{\mathbf{u}}^{n+3/5}$ by $\hat{\mathbf{u}}^{n+3/5}(\xi_1, \xi_2) = \mathbf{u}^{n+3/5}(\xi_1, \eta^n(\xi_1)\xi_2/H)$; $\hat{\mathbf{u}}^{n+3/5}$ is needed to solve problem (26).

At each time step, the subproblems (32)–(34) are solved in the domain Ω^n which is clearly non-polygonal because of the curved portion Γ^n of the boundary. To approximate velocity and pressure we use here an isoparametric version (discussed in, e.g., [2], Chapter 5) of the *Bercovier–Pironneau* finite elements method, also known as the $P_1 - iso - P_2$ and P_1 finite elements approximation. This approximation was introduced in [1] and further discussed in, e.g., [3,4,6,13].

The backward Euler's method has been used to derive the time discretization in (32) and (34). These problems can be seen as a "*generalized*" discrete Stokes problem for which efficient solution methods already exist, as shown in, e.g., [2].

In order to solve the advection step (33) we use a wave-like equation method [2,5,11]: this approach preserves the hyperbolic nature of advection, it introduces low numerical dissipation and it is easy to implement. In particular, we use here a second order accurate time discretization scheme which is discussed in, e.g., [2], Chapter 6, and [11].

We again use the wave-like equation approach to solve the transport problem (26). We observe that (26) does not contain x_1 differentiation of $\hat{\mathbf{u}}$ and therefore the problem reduces to the solution of a family (infinite for the continuous problem, finite for the discrete ones) of transport problems in one space dimension along the vertical direction. Then for $\xi_1 \in (0, L)$, each component of $\hat{\mathbf{u}}$ is the solution of a transport problem of the following form:

$$\begin{cases} \dfrac{\partial \varphi}{\partial t} - a\xi_2 \dfrac{\partial \varphi}{\partial \xi_2} = 0 \quad \text{on } (0, H) \times (t^n, t^{n+1}), \\ \varphi(t^n) = \varphi_0, \\ \varphi(H, t) = b \quad \text{if } a > 0, \quad t \in (t^n, t^{n+1}), \end{cases} \tag{35}$$

with a and b constant with respect to ξ_2 and t. The solution of this problem is discussed in [4].

4. Numerical experiments

We apply the method discussed in Sections 2 and 3 to the numerical simulation of the flow in the downstream section of a slot coater. The basic action of coating is to replace the gas at the surface of a solid substrate by a layer of liquid. Here the substrate is represented by a rigid plane which is translating along the horizontal direction at a fixed velocity $\mathbf{u} = (1, 0)$, as sketched in Fig. 1. The flow of the fluid, initially at rest in the region above this plane, is driven by a constant inlet flow rate and it is subject to capillary forces due to the surface tension at the free boundary $\Gamma(t)$.

The initial configuration of the fluid domain is the rectangle $(L_0, L) \times (0, H)$, with $L_0 = -2$, $L = 8$ and $H = 1$ and an example of the triangulation of the reference domain is reported in Fig. 3. The location of the inlet and outlet sections—which are synthetic boundaries—has been chosen far enough from the interesting region of the flow, that moving such boundaries further outward does not affect the flow solution [12]. The inlet velocity profile is given by

$$\mathbf{u}(L_0, x_2, t) = U(x_2, t)\mathbf{e}_2 = \left(3(1 - 2Q)x_2^2 - 2(2 - 3Q)x_2 + 1\right)\mathbf{e}_2, \tag{36}$$

where Q is the flow rate per unit of width. The inlet velocity profile for $Q = 0.3$ is shown in Fig. 4.

We solve the nonstationary problem and we follow the evolution of the system to a stationary state, which is determined by the following condition

$$\frac{\|\mathbf{u}^n - \mathbf{u}^{n-1}\|_{L^2(\Omega^n)}}{\|\mathbf{u}^n\|_{L^2(\Omega^n)}} < 10^{-7}. \tag{37}$$

In our numerical experiments, the boundary condition in (4) has the following form

$$\mathbf{g}_0 = \begin{cases} \mathbf{0} \quad \text{for } L_0 \le x_1 \le 0, \quad x_2 = H \\ (U(x_2, t), 0) \quad \text{for } x_1 = L_0, \quad 0 \le x_2 \le H \\ (1, 0) \quad \text{for } L_0 \le x_1 \le L, \quad x_2 = 0. \end{cases} \tag{38}$$

The values used for density, viscosity, surface tension and flow rate are $\varrho = 1$, $\mu = 1$, $s = 10$ and $Q = 0.3$, respectively. An indicator of the relative effect of viscous forces versus surface tension acting at the free surface, is the capillary number, defined as $Ca = \mu V/\sigma$, where V is a characteristic velocity. Choosing $V = 1$ as the velocity of the translating plane, the

Please cite this article in press as: G. Guidoboni, et al., Operator splitting for the numerical solution of free surface flow at low capillary numbers, Journal of Computational and Applied Mathematics (2008), doi:10.1016/j.cam.2008.10.051

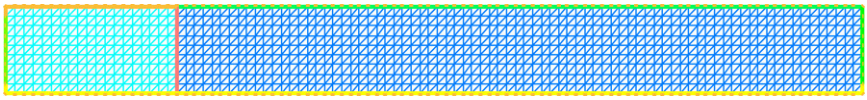

Fig. 3. Pressure mesh in the initial configuration of the flow domain.

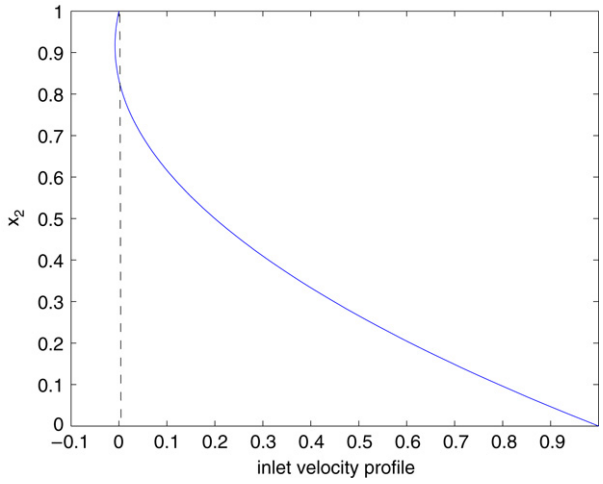

Fig. 4. Inlet velocity profile corresponding to $Q = 0.3$.

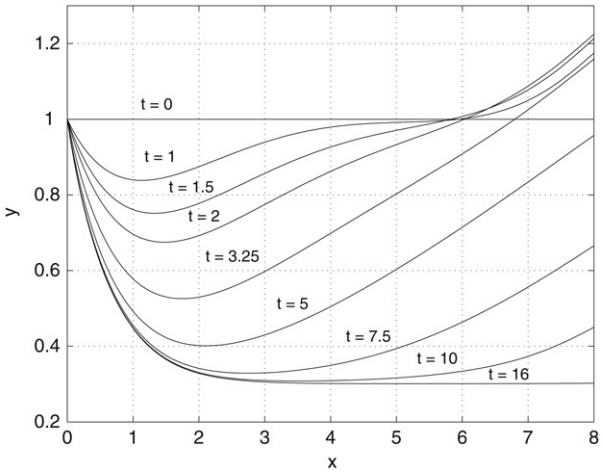

Fig. 5. Time evolution of the profile of the free surface for $\varrho = 1, \mu = 1, s = 10, Q = 0.3$.

capillary number for the case considered here is $Ca = 0.1$, which indicates that the interfacial forces due to the surface tension are stronger than the viscous forces in the flow.

The time evolution of the free surface profile is sketched in Fig. 5, while the streamlines of the flow at various instants of time, more precisely $t = 0.25, 0.75, 1.5, 2, 3.5, 10.25$, are portrayed in Fig. 6. The system reaches a steady state, and the steady profile of the free surface is represented by the solid line in Fig. 7. In the same picture, we compare our steady profile with the steady profile computed with a monolithic algorithm [12] (and tested against earlier results, e.g., [14]) for the same values of the parameters. The agreement between the results is very satisfactory.

The results presented here have been obtained for $h_p = 1/80$, $h_v = 1/160$, $\Delta t = 5 \times 10^{-4}$ and $\tau = \Delta t/5$, where h_p and h_v are the size of the meshes used for pressure and velocity, Δt is the time step and τ is the time sub-step used for the advection sub-problems. The results of these simulations have been tested with $h_p = 1/120$, $h_v = 1/240$, $\Delta t = 2.5 \times 10^{-4}$ and $\tau = \Delta t/5$, and we obtained essentially the same steady free surface profile.

Please cite this article in press as: G. Guidoboni, et al., Operator splitting for the numerical solution of free surface flow at low capillary numbers, Journal of Computational and Applied Mathematics (2008), doi:10.1016/j.cam.2008.10.051

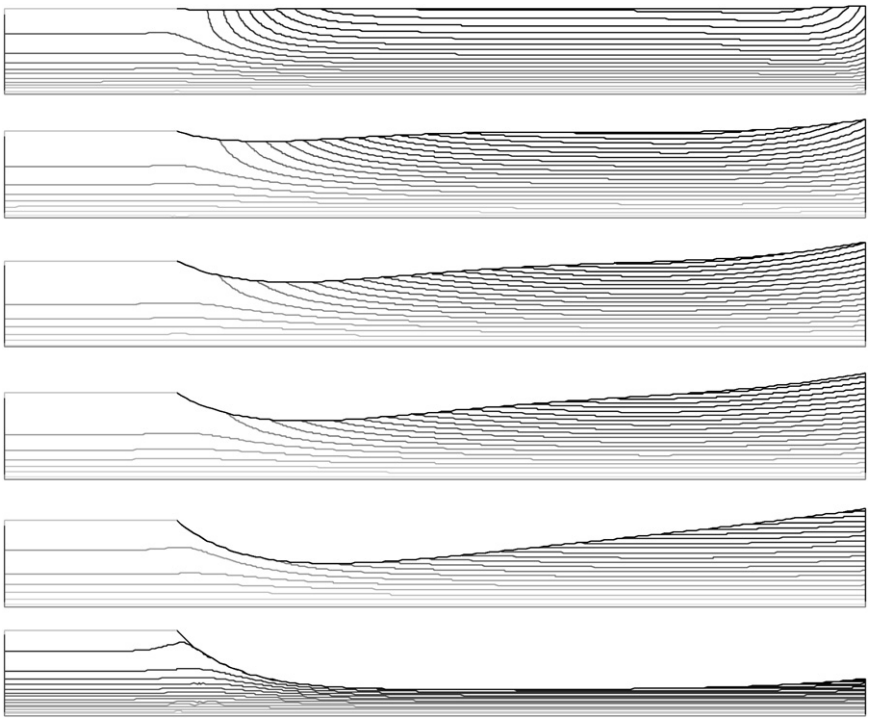

Fig. 6. Streamlines computed for $t = 0.25, 0.75, 1.5, 2, 3.5, 10.25$.

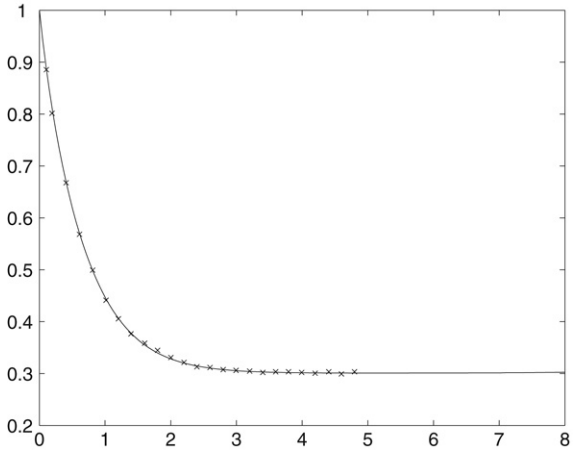

Fig. 7. Comparison between the steady profile of the free surface computed with a monolithic algorithm [12] (*crosses*) and the profile obtained with the splitting algorithm described in this paper (*solid line*) for $Q = 0.3$ and $Ca = 0.1$—i.e., $\varrho = 1$, $\mu = 1$, $s = 10$.

Acknowledgments

This work was supported by the Texas Higher Education Board under ARP grant number 003652-0051-2006 (to GG), by NSF/NIGMS grant number DMS-0443826 (to RG), by NSF/CTS-ITR-0312764 and NSF/CTS-CAREER-0124389 (to MP), and by the NSF/DMS-0811138 (to GG, RG and MP).

References

[1] M. Bercovier, O. Pironneau, Error estimates for finite element method solution of the stokes problem in primitive variables, Numer. Math. 33 (1979) 211–224.
[2] R. Glowinski, in: P.G. Ciarlet, J.-L. Lions (Eds.), Finite Element Methods for Incompressible Viscous Flow, vol. IX, North-Holland, Amsterdam, 2003.
[3] R. Glowinski, E.J. Dean, G. Guidoboni, H.L. Juarez, T.-W. Pan, Applications of operator-splitting methods to the direct simulation of particulate and free-surface flows and to the numerical solution of the two-dimensional elliptic Monge–Ampere equation, Japan Journal of Industrial and Applied Mathematics 25 (2008) 1–63.

Please cite this article in press as: G. Guidoboni, et al., Operator splitting for the numerical solution of free surface flow at low capillary numbers, Journal of Computational and Applied Mathematics (2008), doi:10.1016/j.cam.2008.10.051

[4] R. Glowinski, G. Guidoboni, Hopf bifurcation in viscous incompressible flow down an inclined plane: A numerical approach, J. Math. Fluid Mech. 10 (2008) 434–454.
[5] R. Glowinski, G. Guidoboni, T-W Pan, Wall-driven incompressible viscous flow in a two-dimensional semi-circular cavity, J. Comput. Phys. 216 (1) (2006) 76–91.
[6] R. Glowinski, L.H. Juárez, Finite element method and operator splitting for a time-dependent viscous incompressible free surface flow, Comput. Fluid Dyn. J. 12 (3) (2003) 459–468.
[7] P.M. Gresho, R.L. Sani, Incompressible Flow and the Finite Element Method: Advection-Diffusion and Isothermal Laminar Flow, Wiley, Chichester, New York, 1999.
[8] S.F. Kistler, P.M. Schweizer, Liquid Film Coating: Scientific Principles and their Technological Implications, Chapman & Hall, 1997.
[9] S.F. Kistler, L.E. Scriven, Coating flows, in: J.R.A. Pearson, S.M. Richardson (Eds.), Computational Analysis of Polymer Processing, Applied Science Publishers, London, 1983, pp. 243–299.
[10] G.I. Marchuk, Splitting and alternating direction methods, in: P.G. Ciarlet, J.-L. Lions (Eds.), in: Handbook of Numerical Analysis, vol. I, North-Holland, Amsterdam, 1990, pp. 197–462. (Chapter 3).
[11] T.W. Pan, R. Glowinski, A projection/wave-like equation method for the numerical simulation of incompressible viscous fluid flow modeled by the Navier-Stokes equations, Comput. Fluid Dyn. J. 9 (2) (2000) 28–42.
[12] M. Pasquali, L.E. Scriven, Free surface flows of polymer solutions with models based on conformation tensor, J. Non-Newtonian Fluid Mech. 108 (2002) 363–409.
[13] O. Pironneau, in: P.G. Ciarlet, J.-L. Lions (Eds.), Finite Element Methods for Fluids, J. Wiley, Chichester, 1989.
[14] W.J. Silliman, Viscous film flows with contact lines: finite element simulation, A Basis for Stability Assessment and Design Optimization, Ph.D. Thesis, University of Minnesota, Minneapolis, MN, 1979. Available from UMI, Ann Arbor, MI, order number 7926172.
[15] R.I. Tanner, Engineering Rheology, 2nd edition, Oxford University Press, 2000.

Please cite this article in press as: G. Guidoboni, et al., Operator splitting for the numerical solution of free surface flow at low capillary numbers, Journal of Computational and Applied Mathematics (2008), doi:10.1016/j.cam.2008.10.051